ICES Journal of Marine Science, 2026, Vol. 83, Issue 1, fsaf225
https://doi.org/10.1093/icesjms/fsaf225
Received: 19 August 2025; **revised:** 26 November 2025; **accepted:** 27 November 2025
Original Article

Informing krill fishery management through modelling spatial distribution and diet of a major krill predator, mackerel icefish (*Champsocephalus gunnari*), at South Georgia

Timothy Jones*, Victoria Warwick-Evans, Simeon L. Hill, Martin A. Collins

British Antarctic Survey, NERC, High Cross, Madingley Road, Cambridge CB3 0ET, United Kingdom

*Corresponding author. British Antarctic Survey, NERC, High Cross, Madingley Road, Cambridge CB3 0ET, United Kingdom. E-mail: times@bas.ac.uk

Abstract

Demersal fish are a critical component of Antarctic marine ecosystems and may consume large quantities of Antarctic krill (*Euphausia superba*), placing them at risk from competition with commercial krill fishing. However, estimating relative overlap between krill fishing and consumption by demersal fish is beset by uncertainty regarding fish distribution and diet. In this study, we develop models of mackerel icefish (*Champsocephalus gunnari*) distribution and diet around the subantarctic island of South Georgia to predict the distribution of krill consumption attributable to mackerel icefish to aid in krill fishery spatial management. We use trawl survey data (1986–2023) to construct distribution models for mackerel icefish biomass across the South Georgia and Shag Rocks shelf. Using gut content data, we also developed spatial models for the proportion of krill in mackerel icefish diets, allowing for a novel evaluation of spatial variation in potential krill availability. Models indicated that mackerel icefish are distributed across the South Georgia and Shag Rocks shelves to 400 m depth, with high density areas towards the shelf edge associated with seafloor topography. Spatial variation in diet was evident between South Georgia, where krill predominated, and Shag Rocks, where diets were more piscivorous. Higher krill diets along the South Georgia shelf edge were also coincident with elevated icefish density, suggesting that icefish distribution and diet may be associated with krill availability. Spatial variation in krill consumption by mackerel icefish suggests that overlap with the krill fishery is currently low despite mackerel icefish being a major krill consumer. However, estimates of mackerel icefish biomass and total krill consumption were uncertain due to uncertainties surrounding icefish catch and feeding rates, and were likely negatively biased due to the inability to account for the unknown proportion of fish in the water column that are unavailable to trawl sampling. Despite those concerns, our results provide the foundation for including demersal fish information in spatial management of the krill fishery.

Keywords: Antarctic fish; Antarctic krill; ecosystem-based management; prey consumption; spatial overlap analysis; species distribution model

Introduction

Given rising human demand for marine food resources (Naylor et al. 2021), there is an increasing need to balance fisheries extraction against the potential ecosystem impacts that may arise due to increased fishing (Pauly et al. 2005, Petza and Katsanevakis 2024). Setting regional quotas based on ecosystem requirements is one important aspect (Hill et al. 2020); however, many studies have demonstrated that management is often applied at spatial scales that are inappropriate both with regards to ecosystem processes (Watters et al. 2020, Berger et al. 2021) and the realized spatio-temporal distribution of fishing effort (Warwick-Evans et al. 2022a, Bertrand et al. 2012). Understanding the spatial arrangement of fishing and the variety of ecosystem processes that may be impacted by fishing is therefore a requirement for effective ecosystem-based management (Falco et al. 2022).

One such consideration is understanding the relative overlap between consumption by predators and projected or realized fishing effort (Warwick-Evans et al. 2022b, Bertrand et al. 2012). This is particularly important for forage species (e.g. small pelagic fish and krill) as they frequently support multiple upper-trophic species (Griffiths et al. 2013) but are often patchily distributed (Santora et al. 2014), such that aggregations may be targeted on multiple fronts. Minimizing the potential for competition with predators and/or localized depletion of resources by fisheries (Bertrand et al. 2012) therefore requires that management actions are informed by an understanding of the distribution of consumption by predators (Santora et al. 2014). Not only does this require information on the spatial distribution of predators (Warwick-Evans et al. 2022b, Ratcliffe et al. 2021), but also how predator diets vary among locations depending on prey availability (Wells et al. 2024).

Antarctic krill (*Euphausia superba*, hereafter krill) are an important link in the Southern Ocean food web, providing a vital prey resource for many predator species (Murphy et al. 2007). They are also the target species for the largest fishery, measured by catch, in the Southern Ocean, which is primarily concentrated in the southwest Atlantic (Nicol and Foster 2016, Trathan et al. 2025). The Commission for the Conservation of Antarctic Marine Living Resources (CCAMLR), who are responsible for managing the krill fishery, had previously set catch limits within large-scale subareas (shown in Fig. 1) in the southwest Atlantic (CCAMLR area 48). However, over recent years, krill fishing has become increasingly concentrated in space and time within those subareas, poten-

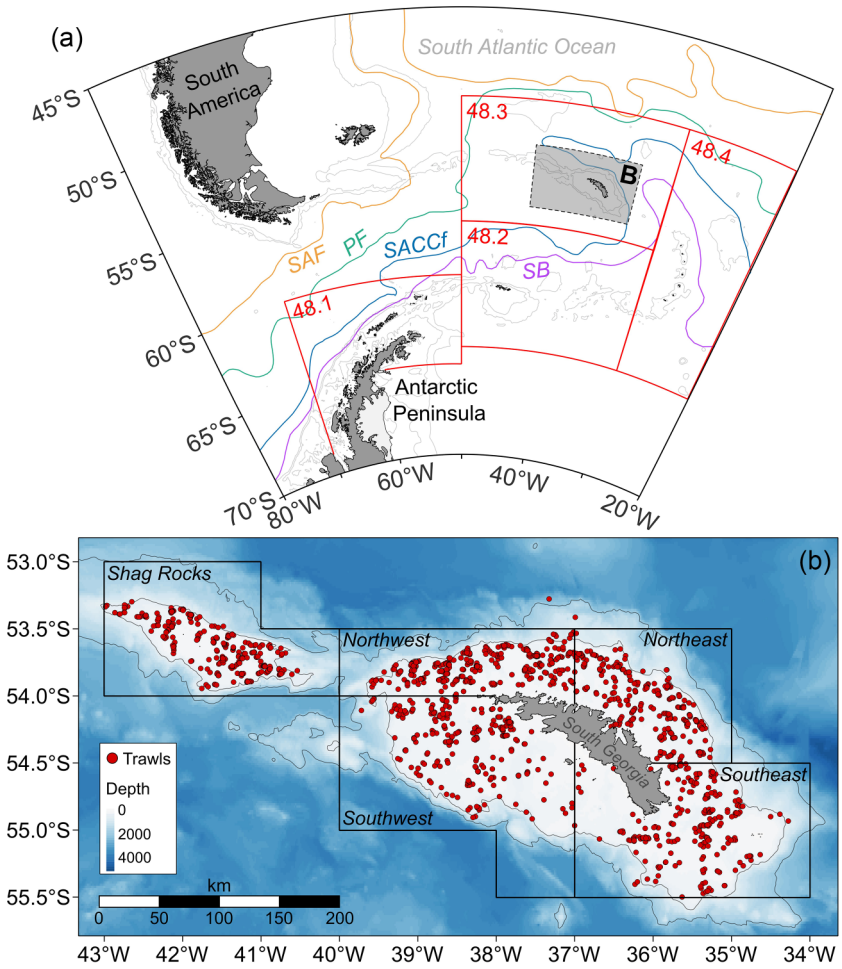

Figure 1. Map of the study region (**A**) in the southwest Atlantic Ocean in relation to South America and Antarctica and proximity to oceanographic features (SAF = Subantarctic Front, PF = Polar Front, SACCf = Southern Antarctic Circumpolar Current Front, SB = southern boundary of the Antarctic Circumpolar Current). Boundaries of CCAMLR Subarea management units (48.1, 48.2, 48.3, 48.4) are also shown. Map showing the South Georgia and Shag Rocks shelf (**B**) indicating trawl locations from groundfish surveys (1986–2023) used throughout analyses in relation to bathymetry, with polygons indicating sectors used in sampling stratification. Contour lines represent the 500 m and 2000 m isobaths.

tially increasing the risk to krill-dependent predators (Watters and Hinke 2022). Recognising this, in 2019 CCAMLR began developing a management approach to apportion catch among smaller-scale management units within those subareas (CCAMLR 2019, paragraphs 5.17 to 5.19). A key requirement of this approach is understanding krill distribution and consumption by predators at a relatively fine spatial scale (Constable et al. 2023). Despite plans to implement this approach, the CCAMLR conservation measure that divided the catch limit of 620 000 tonnes among those four subareas (CM 51–07) expired at the end of 2024, leading to the absence of subarea-level spatial management during the 2024/25 fishing season (Trathan et al. 2025). Given that, identification of foraging patterns of krill-dependent predators may be a necessary component informing future negotiations surrounding the krill fishery as a prerequisite for establishing a data-informed approach to spatial management.

Although the krill fishery tends to focus around the Antarctic Peninsula and South Orkney Islands, it frequently moves to South Georgia (Fig. 1) during winter (Trathan et al. 2021). Krill abundance varies significantly within- and among-seasons at South Georgia linked to transport and retention from Antarctica (Murphy et al. 2004, Reid et al. 2010, Fielding et al. 2014). South Georgia is also a haven for wildlife, providing important breeding and feeding grounds for numerous marine predators (Boyd 2002, Trathan et al. 2021). As such, understanding the spatial distribution of krill predators at South Georgia is fundamental if we are to manage the krill fishery in a precautionary manner.

While multiple studies have investigated the fine-scale spatial distribution of krill consumption by penguins, seals, and cetaceans (Warwick-Evans et al. 2018, 2022a, 2022b), fewer studies have taken a similar approach to demersal fish (although see Canseco et al. 2024). Demersal fish are an important part of the krill-based ecosystem in the Southern Ocean, potentially accounting for > 70% of krill consumption in some areas (Hill et al. 2007). Mackerel icefish (*Champsocephalus gunnari*, henceforth referred to as icefish) are the dominant demersal fish species at South Georgia and are highly dependent on krill (Reid et al. 2005, Main et al. 2009). A member of the Antarctic icefish family (Channicthyidae), mackerel icefish are distributed around Subantarctic islands to depths of ~ 700 m and are bentho-pelagic, being highly adapted to feed on krill in the water column (Kock and Everson 1997, Kock 2005). Given their high abundance and reliance on krill, ecosystem models suggest they are potentially

Table 1. Summary of bottom-trawl surveys used in analyses of mackerel icefish (Champsocephalus gunnari) distribution and diet.

Survey	Date start	Date end	Gear	Design	Trawls	Prev. (%)	CPUE (kg/km^2)	Diet samples	
								Trawls	Fish
SG87	29-Nov-86	17-Dec-86	B-454 OT	SRS	104	98	1370		
SG88	19-Dec-87	12-Jan-88	P32/36 OT	SRS	112	98	429		
SG89	1-Feb-89	14-Feb-89	P32/36 OT	SRS	55	91	928		
SG90	6-Jan-90	26-Jan-90	HC120 OT	SRS	68	85	19 570		
SG91	22-Jan-91	11-Feb-91	FP120	SRS	77	91	773		
SG92	3-Jan-92	26-Jan-92	FP120	SRS	81	94	1047		
SG94	4-Jan-94	8-Feb-94	FP120	SRS	81	95	541		
SG97	2-Sep-97	29-Sep-97	FP120	SRS	55	96	2057		
SG00	16-Jan-00	30-Jan-00	FP120	SRS	41	95	1185		
SG02	12-Jan-02	1-Feb-02	FP120	SRS	63	97	1095		
SG03	7-Jan-03	31-Jan-03	FP120	RAD	38	37	909		
SG04	7-Jan-04	5-Feb-04	FP120	SRS	64	75	2309	46	584
SG05	7-Jan-05	25-Jan-05	FP120	SRS	42	76	248	30	433
SG06	3-Jan-06	1-Feb-06	FP120	SRS	66	83	3810	52	1176
SG07	27-Aug-07	21-Sep-07	FP120	SRS	49	88	2787	38	441
SG08	16-Apr-08	30-Apr-08	FP120	SRS	70	87	2417	51	733
SG09	15-Jan-09	23-Jan-09	FP120	SRS	73	93	1551	57	828
SG10	15-Jan-10	24-Jan-10	FP120	SRS	75	95	2298	66	1162
DW10	29-Jan-10	31-Jan-10	FP120	DW	6	0	0		
SG11	26-Jan-11	6-Feb-11	FP120	SRS	87	95	1629		
SG12	26-Jan-12	29-Jan-12	FP120	SRS[a]	22	91	11 627	18	367
SG13	22-Jan-13	29-Jan-13	FP120	SRS	68	98	11 312	56	805
SG15	13-Jan-15	23-Jan-15	FP120	SRS	77	91	1672	67	1094
SG17	30-Jan-17	7-Feb-17	FP120	SRS	72	99	3967	69	1380
DW19	5-Feb-19	5-Feb-19	FP120	DW	3	0	0		
SG19	27-Jan-19	5-Feb-19	FP120	SRS	73	97	1489	68	1190
SG21	8-May-21	28-May-21	FP120	SRS	76	92	334	61	713
SG23	1-Feb-23	10-Feb-23	FP120	SRS	75	95	1866	63	876
				Totals	**1773**	**91**	**2750**	**742**	**11 782**

[a]: incomplete survey; only Shag Rocks and the NW South Georgia shelf were sampled.
Trawl sample size (n), prevalence (% of trawls with catch > 0) and gross mean catch per unit effort (CPUE = catch/trawl area swept) are given along with sample sizes for fish sampled for diet analyses. All values presented are after data-cleaning and represent sample sizes entering analyses. Design abbreviations: SRS = stratified random sample, RAD = radial, DW = deepwater trawl surveys. See Supplementary materials for information on gear configuration.

responsible for 8%–27% of all krill consumption on the South Georgia shelf, exceeding consumption by any other groundfish species there (Hill et al. 2012). In addition, mackerel icefish were historically overexploited at South Georgia (Kock 2005), and evidence suggests that populations have not fully recovered to pre-exploitation levels (Reid et al. 2005). Management of the krill fishery at South Georgia should therefore aim to avoid any potential adverse impacts to mackerel icefish and to allow the population to develop according to their ecological potential given current availability of prey resources.

Here, we use a series of models fitted to catch and diet data from trawl surveys to estimate the long-term average spatial distribution of icefish and their consumption of krill around South Georgia (Fig. 1). We had three main objectives. We first aimed to predict the average distribution of icefish within this region. This was achieved using hurdle models fitted to demersal trawl catch data and informed by environmental covariates to identify factors related to patterns of occurrence and biomass. Secondly, we aimed to identify spatial variation in diet composition, which we investigated using stomach content data from trawl surveys (2004 onwards), to better understand spatial variation in the availability of alternate prey resources and to inform krill consumption estimates. Finally, we aimed to combine results from distribution model and diet analyses to estimate consumption of krill by icefish within this region, and to identify the relative overlap with the krill fishery. The resulting estimates of icefish distribution and krill consumption will help facilitate the development of an evidence-based management strategy for the krill fishery at South Georgia.

Methods

Groundfish survey data

Trawl surveys

Data on icefish distribution at South Georgia (Fig. 1) were collected during 28 demersal trawl surveys from 1986 to 2023 (Table 1). Sampling consisted of 30-minute trawls carried out predominantly during daylight (94% between nautical twilight at dawn/dusk, n = 1773) at a speed of 3–4 knots, using similar gear throughout (trawl dimensions: 16-22 m wingspread, 3-6 m headline height; detailed in *Supplementary materials: Section 1*). Surveys were usually during the austral summer (November-February), except for 1997 and 2007 (August-September), and 2008 and 2021 (April-May; Table 1). Trawl locations were chosen according to a stratified random-design across sectors and depth zones (100–200 m, 201–350 m, > 350 m; Fig. 1), except for during deepwater surveys in 2003, 2010 and 2019 where a limited number of trawls were performed (Fig. S1, where S denotes figures in *Supplementary materials*). All trawls were retained for analysis, except for trawls hauled early (duration < 15 minutes) due to unsuitable ground or gear failure. Total icefish weight (kg) was recorded for each trawl in addition to depth, distance, and

Table 2. Trawl-specific and habitat covariates, along with data sources, for variables (units in parentheses) considered in mackerel icefish (Champsocephalus gunnari) distribution models.

Variable	Source
survey: Survey categorical variable	survey
date: Survey mid-point date	survey
sun: Sun altitude above the horizon (radians)	trawl
east: Easting of trawl mid-point (m)[a]	trawl
north: Northing of trawl mid-point (m)[a]	trawl
depth: Bathymetric depth (m)[b]	ETOPO 2022 | Res: 0.0167°
slope: Seafloor slope (unitless)	
curve: Planform curvature of seafloor (unitless)	
SST.mean: Mean sea surface temperature (°C) [Surf.]	Global Ocean OSTIA SST (product: sst_glo_sst_l4_rep_observations_010_011) Time: 1981–2023 (daily) | Res: 0.05°
SST.sd: Std. dev. of sea surface temperature (°C) [Surf.]	
SSal.mean: Mean sea surface salinity (PSU) [Prod.]	Global Ocean Physics Reanalysis (product: global_multiyear_phy_001_030) Time: 1993–2023 (daily) | Res: 0.083°
SSal.sd: Std. dev. of sea surface salinity (PSU) [Surf.]	
FTemp.mean: Mean temperature near seafloor (°C) [Floor]	
FSal.mean: Mean salinity near seafloor (PSU) [Floor]	
FSal.sd: Std. dev. of seafloor salinity (PSU) [Floor]	
FVel.mean: Mean current speed near seafloor (ms^{-1}) [Curr.][c]	
SVel.mean: Mean surface current speed (ms^{-1}) [Curr.][c]	
EKE.mean: Mean eddy kinetic energy (m^2s^{-2}) [Curr.][c]	
MLT.mean: Mean mixed layer thickness (m) [Prod.]	
CHL.mean: Mean surface chlorophyll-a concentration (mg m^{-3}) [Prod.]	Global Ocean Colour (product: oceancolour_glo_bgc_l4_my_009_104) Time: 1997–2023 (daily) | Res: 4km
FDO2.mean: Mean dissolved oxygen near seafloor (mmol m^{-3})	Global Ocean Biogeochem. Hindcast (product: global_multiyear_bgc_001_029) Time: 1993–2023 (daily) | Res: 0.25°

[a]: Trawl mid-points were converted from latitude-longitude (decimal degrees) to easting-northing (m) according to the Lambert azimuthal equal-area projection centered on South Georgia.
[b]: In-situ depth measurements were used in model fitting, whereas depth from bathymetry data was used to predict icefish distribution.
[c]: Derived from zonal and meridional components of current velocity.
Covariate categories (Surf. = surface temperature and salinity; Floor = seafloor temperature and salinity; Prod. = surface productivity; Curr. = current velocity) assigned based on collinearity ($0.55 < |r| < 0.8$) are given in [], and only one variable per group permitted to appear in any given model. Dataset sources, including Copernicus Marine Data Store product ID, temporal coverage and spatial resolution are also given. All environmental datasets were obtained for the area within the 2000 m isobath around South Georgia and Shag Rocks (33–44°W, 52.5–56°S), to encompass trawl locations.

horizontal opening (wingspread). Weights were converted to catch per unit effort (CPUE) with effort equal to area swept (trawl distance × wingspread; km^2).

Diet data

Since 2004, whole stomach samples were retained from a random sample (typically ≤ 30) of icefish per haul (Table 1). Stomach contents were identified to the lowest possible taxonomic resolution, then counted and weighed for each prey taxon for each icefish sampled. Composition by mass was used throughout as a measure of proportional consumption.

Distribution models for mackerel icefish density

Bathymetric and environmental covariates

Icefish distribution models were constructed based on trawl CPUE (kg/km^2) in relation to spatial and environmental covariates (Table 2). Bathymetric data were obtained from the ETOPO 2022 dataset (NOAA 2022). These data were also used to calculate slope (terrain function in the raster package; Hijmans 2025), and planform curvature (curvature function in the spatialEco package; Evans and Murphy 2023), which quantifies curvature perpendicular to the prevailing slope as an indicator of seafloor grooves (negative curvature) and ridges (positive curvature). Slope and planform curvature were calculated at a spatial scale of 10 km.

Environmental data were obtained from the Copernicus Marine Data Store, and included temperature, salinity, current magnitude, and dissolved O_2 concentration at the surface and near the seabed, and eddy kinetic energy (EKE), mixed layer thickness and surface chlorophyll-a concentration (Table 2). These variables were chosen as they may effect icefish distribution directly (i.e. via temperature limitation; Kock 2005) or indirectly via their effects on icefish prey. Environmental datasets were processed into maps representing the average climatological mean and variability (standard deviation calculated across layers each year then averaged across years, thereby representing average intra-annual variation) across data from 1993 (1997 for chlorophyll-a) to 2023. We initially considered predictors based on season-specific climatologies (i.e. December-February) given differences in survey-timing. However, we chose to use year-round averages as they were highly correlated with seasonal averages, and to avoid spurious relationships arising from the inclusion of covariate values derived only from winter surveys that had limited representation (four surveys). Values for each covariate were then extracted according to trawl mid-point location. Habitat covariates that were highly skewed were transformed, and all were scaled prior to analysis. The covariate set was then reduced by excluding variability covariates that were highly collinear (correlation coefficient; $r = 0.8–0.98$; Dormann et al. 2013) with the mean of the same variable (Fig. S2) to avoid multicollinearity. Furthermore, covariate combinations that were moderately collinear ($0.55 < |r| < 0.8$) were grouped (Table 2) and trialed against each other, rather than included together, to identify the best model while minimizing multicollinearity.

Hurdle model framework

Distribution models were constructed following a two-stage hurdle modelling approach. This approach was chosen to firstly identify factors related to icefish occurrence (presence-absence component), and to separately identify factors associated with the spatial distribution of biomass within their range (non-zero CPUE component). Presence-absence models were fitted to a binary response (CPUE > 0 set to 1; binomial distribution, logit link), and CPUE models were fitted to log-transformed CPUE, excluding absence records (normal distribution). Analyses were performed using generalized additive models (GAMs) fitted using gam in the mgcv package in R (Wood 2011). Unless stated, all smooths were thin-plate regression splines with a shrinkage penalty (smooth type = "ts"), such that non-informative terms shrink to 0, effectively removing them from the model (Marra and Wood 2011).

Several terms were included in each model to account for sampling differences among trawls. A smooth for date and survey random effects were included to model long-term trends and interannual variability, respectively. Time of day was also included via a smooth based on sun altitude (x = 0 at dawn, x = $\pi/2$ at zenith) to account for differences in CPUE throughout the day that may occur as a result of diel vertical movement (Kock 2005).

Spatial variability in icefish distribution was modelled via smooth terms for environmental and bathymetric covariates (henceforth, habitat covariates; Table 2), and a spatial field dependent on location (easting, northing) to account for unexplained spatial variation. Spatial effects were specified as a Gaussian-process (basis = "gp") smooth which are parameterized by a range parameter that controls the extent of spatial continuity (Kammann and Wand 2003). We investigated range parameters from 5 km to 60 km in 5 km increments, and only permitted stationary fields (i.e. no continuous trend) to favour the explanation of large-scale gradients via habitat covariates.

Fitted models consisted of smooth terms for bathymetric covariates (depth, slope, planform curvature), along with smooths for one variable from each habitat covariate set (Table 2), plus a spatial field. Selection among alternate models (habitat covariates, range parameter) was achieved by fitting all possible models and ranking them based on AIC and cross-validated predictive accuracy (see *Supplementary materials: Section 2*). For presence-absence, predictive accuracy was calculated as sensitivity (% presences correct), specificity (% absences correct), and area under the receiver operating characteristic curve (AUC; Heagerty and Zheng 2005), whilst normalized (relative to standard deviation of observed values) root-mean-squared error (nRMSE; ranges from 0 for a perfect fit, to 1 for no better than an intercept-only model) was used for log-CPUE.

Following fitting, models were validated according to standard GAM diagnostics (residual distribution, homoscedasticity), and those with maximum concurvity greater than 0.8 omitted from further consideration (Wood 2008). Results are presented for the model with lowest predictive error and AIC (ΔAIC < 4).

Density maps

Predicted distribution maps were constructed based on probability of occurrence (presence-absence) and CPUE predicted to a 2 × 2 km grid populated with habitat covariates. Date and sun angle were held constant at their maximum values (date = Jan-2023; sun = 1) so that predictions represent the most recent survey, and are standardized to the same time-of-day.

For CPUE, predictions were calculated as the mean of a log-normal distribution;

$$\widehat{CPUE} = \exp\left(\hat{\mu} + \frac{\hat{\sigma}^2}{2}\right) \quad (1)$$

where $\hat{\mu}$ is expected log-CPUE, and $\hat{\sigma}^2$ is residual variance. Multiplying by the probability of occurrence from the presence-absence model, $\hat{p}$, gives an estimate of density (kg/km^2):

$$\hat{D} = \hat{p} \times \widehat{CPUE} \quad (2)$$

Overall and sector-specific (i.e. Fig. 1B) biomass estimates were also calculated by summing $\hat{D}$ over areas and multiplying by grid-cell area (4 km^2). Uncertainty in spatial density (presented via coefficient of variation; CV) and biomass (95% CI) estimates were quantified using posterior simulation, allowing for uncertainty to be propagated across presence-absence and CPUE model components (see *Supplementary materials: Section 2*). We also investigated whether patterns of icefish density have shifted over time by repeating the analyses to data restricted by time (1987–1997, 2000–2010, 2011–2023). However, given our main aim was to create a long-term average representation of icefish distribution, we present these results in the *Supplementary materials* as validation only.

Given that models were informed by trawl-based CPUE, predictions of density and biomass are likely underestimates due to individuals present throughout the water column (Kock and Everson 1997) above the headline height (3-6 m) of the trawl gear. As such, values for "density" and "biomass" should be interpreted as the catchable density and biomass given the sampling methodology. However, despite this limitation, CPUE is a valid measure of relative abundance among-trawls, and therefore variation among locations.

Proportion of krill in icefish diets

Diet sample processing

Diet sample data were initially processed to account for records of unknown euphausiids (0%–32% of gross mass per year) that may otherwise bias analyses (see *Supplementary materials: Section 3*). Prior to this, the proportion of *Euphausia superba* and unknown euphausiids in stomach content samples was examined in relation to fish size to identify whether reassignment of unknown euphausiids may suffer from bias due to diet size-dependence. However, little variation among sizes were evident in our stomach content data (Fig. S3). Data were then aggregated to trawls given our focus on spatial patterns in diet composition and to avoid pseudo-replication. Trawl-averaged krill proportion was calculated as the summed krill mass divided by the total stomach content mass for all fish sampled per trawl. We also calculated the number and mean length of fish sampled each trawl.

Analyses

Trawl-aggregated krill proportions were analyzed using GAMS fitted using the gamlss package (Rigby and Stasinopoulos 2005) assuming a 0/1 inflated beta distribution

as the response consisted of a mix of continuous proportions, 0's (no krill) and 1's (all krill). Models were constructed by first identifying the best sub-models for variance and 0/1 inflation parameters, which were then fixed throughout subsequent analyses (see *Supplementary materials: Section 4*). For the mean proportion, we considered survey random effects and smooth terms (penalized smooths; basis = "ts") for depth and trawl-averaged fish length, to model interannual variability as well as depth-related and ontogenetic changes in diet, respectively. We chose to model spatial variation using three different approaches, plus a model with no spatial effects, to investigate how resolution of diet information effects consumption estimates. These consisted of spatial variation being modelled either by sector or strata (sector by depth-zone) random effects, which represent relatively coarse resolution of diet composition, or using a gaussian-process smooth to model continuous variation. As with icefish density, alternate spatial smooths (range parameter: 10-60 km in 5 km increments; stationary and non-stationary fields) were trialed. All possible combinations of survey, depth, time, fish length, and spatial effects were evaluated and ranked based on AIC.

Spatial variation in the proportion of krill in icefish diets

Maps representing the long-term mean proportion of krill in icefish diet were created by using models to predict values onto a 2 × 2 km resolution grid as described for icefish distribution. Uncertainty of predicted proportions was quantified using bootstrap resampling (n = 1000) and are presented via 95% CI (area-based means) or CV (spatial predictions).

We also provide gross diet composition (proportion by mass per survey) for South Georgia and Shag Rocks, grouped into: Euphausiids, with sub-categories for *E. superba*, other *Euphausia* spp., and *Thysanoessa* sp., Other Crustaceans, with sub-categories for *Themisto gaudichaudii*, and *Antarctomysis* sp., and Fish, split into Nototheniidae, Channichthyidae, and Myctophidae.

Krill consumption estimates

Daily consumption rate

Daily consumption rates, expressed as a percentage of body mass, were taken from Kock et al. (2012). Given the range of published values for South Georgia (0.3–2.2% body mass per day; Kock et al. 2012), we present estimates assuming rates of 0.5%, 1% and 2% body mass per day.

Spatial distribution and gross estimates of krill consumption

Maps of krill consumption were created by combining density (kg/km^2) and krill dietary proportion layers with relative daily consumption rates (% body mass consumed per day). Given the bias in biomass estimates noted previously, these estimates should be interpreted as consumption attributable to catchable biomass. Furthermore, our analyses do not account for spatial or temporal variation in icefish size. However, we expect any bias associated with this to be relatively small as the proportion of krill in icefish diets seems to vary little among fish sizes (Fig. S3).

Several consumption scenarios were investigated by varying daily consumption rate and spatial representation of icefish diet (static, sector-specific, or continuous). Consumption estimate uncertainty was calculated via bootstrap, by repeatedly drawing alternate density (generated by posterior simulation) and krill proportion (generated by bootstrap) maps to create different realizations (n = 10 000) of krill consumption. These were processed to represent uncertainty in spatial distribution (CV) and area-based estimates (95% CI).

Krill fishery and spatial statistics

Catch data for the krill fishery around South Georgia (2004–2023) were obtained from CCAMLR (Data Request 683), consisting of location and total wet weight of krill per haul. These data were processed into a map representing cumulative catch within 2 × 2 km grid cells using the same grid as used for density. Spatial overlap between the fishery and krill consumption by icefish was calculated using the index of collocation (IoC) that measures the relative (0–1) co-occurrence of two populations (Carroll et al. 2019):

$$IoC = \frac{\sum_i^n \left(p\_catch_i * p\_eaten_i\right)}{\sqrt{\sum_i^n p\_catch_i{}^2 \sum_i^n p\_eaten_i{}^2}} \quad (3)$$

where *p_catch* is fishery catch, and *p_eaten* is consumption by icefish in grid-cell *i* relative to their respective totals. Spatial overlap was assessed for each diet scenario (static, sector-specific, continuous spatial variation) to examine sensitivity to alternate representations of diet. This approach identifies the overlap between two average distributions (mackerel icefish, krill fishery), and therefore does not account for interannual variability in distributions. To address potential changes in fishery distribution, we also created equivalent maps of cumulative krill catch in 5-year blocks from 2004 to 2023 and compared the resultant distributions.

All analyses were performed in R v4.3.3 (R Core Team 2024).

Results

Presence-absence model results

Overall, mackerel icefish were caught in 91% of all trawls (n = 1773), varying from 75%–99% among regular surveys (Table 1). The best-fitting model for icefish presence-absence contained depth, seafloor slope and planform curvature, and seafloor dissolved oxygen (DO) concentration, along with a 25 km range spatial field (Table 3). Effects of other covariates were all shrunk to zero (EDF ≈ 0) indicating no effect (Table S4). Predictive accuracy calculated via cross-validation was high for sensitivity (99%) and AUC (0.94), but specificity was relatively lower (54%; Table 3).

Fitted probabilities displayed a non-linear relationship with depth, reaching values above 0.9 from 90–300 m, and declined to less than 0.1 for depths greater than 510 m (Fig. 2). Negative relationships were estimated for seabed slope and curvature (Fig. 2), indicating higher probability of occurrence in areas with low slope and negative curvature, such as submarine canyons. Seafloor DO was positively correlated with occurrence, although fitted effects were weak and highly uncertain. Spatial effects indicated higher probability across the South Georgia shelf compared to Shag Rocks, except for the central portion of the northern South Georgia shelf (lower) and towards the centre of Shag Rocks (higher; Fig. 2).

Catch per unit effort—model results

Survey-averaged CPUE varied considerably among surveys, ranging from 248 kg/km^2 (2005), to more than

Table 3. Performance of models used to estimate mackerel icefish (Champsocephalus gunnari) distribution.

Presence-absence					
Model	**AIC**	**D^2**	**Sens.**	**Spec.**	**AUC**
depth [2.7] + slope [1.1] + curve [1.0] + FDO2.mean [0.7] + space(25 km) [18.2]	498.3	62.3	98.5	54.3	0.940
Log-CPUE					
Model	AIC	D^2	nRMSE		
depth [3.5] + slope [0.6] + SST.sd [3.3] + space(15 km) [36.4] + sun [1.0]	6475.8	30.2	0.877		
depth [3.5] + slope [0.6] + SST.sd [3.3] + SSal.mean [0.2] + space(15 km) [36.2] + sun [1.0]	6478.4	30.2	0.878		
depth [3.5] + slope [0.3] + FTemp.mean [2.2] + SST.sd [3.1] + space(15 km) [35.4] + sun [1.0]	6479.2	30.4	0.878		
depth [3.5] + slope [0.6] + FTemp.mean [2.4] + space(15 km) [38.8] + sun [1.0]	6479.6	30.2	0.877		
depth [3.5] + slope [0.7] + SST.sd [3.3] + MLT.mean [0.3] + space(15 km) [36.0] + sun [1.0]	6480.2	30.2	0.879		
depth [3.5] + slope [0.5] + SST.sd [3.3] + EKE.mean [0.2] + space(15 km) [36.4] + sun [1.0]	6480.3	30.3	0.878		
depth [3.5] + slope [0.5] + SST.sd [3.3] + EKE.mean [0.6] + MLT.mean [0.7] + space(15 km) [35.2] + sun [1.0]	6480.4	30.2	0.880		
depth [3.5] + slope [0.5] + FTemp.mean [2.3] + SST.sd [3.1] + MLT.mean [0.7] + space(15 km) [34.0] + sun [1.0]	6480.5	30.3	0.879		

Model statistics include Akaike's Information Criterion (AIC), deviance explained (D^2), and predictive statistics assessed via 10-fold cross-validation of sensitivity, specificity, and area under the receiver operating characteristic curve (AUC) for the presence-absence component, and normalized root-mean-squared error (nRMSE) for the CPUE component. Results are given for the optimal (lowest AIC) spatial range (given in parentheses) for each of the presence-absence and CPUE components and for each model with $\Delta AIC < 5$. Estimated degrees of freedom (EDF) of model smooths are given in []. Covariate smooths included in models but had EDF < 0.1 are not included in model formula, and alternate models (different covariates) that functionally resulted in the same model due to shrinkage are only represented once. All models contained survey random effects in addition to those indicated.

10,000 kg/km^2 (1990, 2013), but typically (13 of 25 standard surveys) ranged from 1000 to 2500 kg/km^2 (Table 1). The model with lowest AIC for log-CPUE contained depth and seabed slope, variation in SST, and a spatial smooth with 15 km range (Table 3). Predictive error varied little among models with range parameters between 10-20 km (nRMSE = 0.877–0.880; Table S5) and was relatively high, indicating much unexplained variation.

Catch-per-unit effort displayed a unimodal relationship with respect to depth, with highest CPUE (above 90% of the peak value) predicted at 160-210 m depth and falling below 10% of the maximum for depths greater than 350 m (Fig. 2). The third and fourth ranked models ($\Delta AIC = 3.4–3.7$) also contained a non-linear effect of mean seafloor temperature (Table 3). Both temperature covariates displayed unimodal relationships, with highest CPUE predicted for locations with near regional average seafloor temperatures (~1.5°C) and at locations with moderate variation in SST (Fig. 2). Inclusion of seafloor slope suggested abundance decreases with increasing slope, although uncertainty for this effect was high (Fig. 2). Mixed layer thickness (MLT), surface salinity, and eddy kinetic energy (EKE) were also variously included across high-ranking models (Table 3). However, these terms only had minor effects (EKE and MLT: negative; surface salinity: very weakly positive) with confidence intervals that overlapped with zero throughout the covariate range.

Fitted spatial smooths were indicative of higher density towards the shelf edge around South Georgia, and at the center of Shag Rocks (Fig. 2). Models also estimated a positive relationship between CPUE and sun angle, equivalent to average CPUE being 51% (95% CI: 16%–98%) higher at midday compared to dawn. To investigate daily patterns further, we also created an equivalent model to the best-fitting model for CPUE, but replacing sun altitude with time-of-day expressed as minutes since midnight. The alternate model indicated higher CPUE at midday, with lower values either side of this being approximately symmetric (Fig. S9), consistent with results from the model containing sun altitude. Both models had equivalent deviance explained, but the model containing sun altitude had lower AIC ($\Delta AIC = -1.86$).

Subsequent analyses are based on the best-predicting model for each of presence-absence and CPUE (Table 3).

Spatial variation in mackerel icefish density

Predicted icefish occurrence was high (> 0.95) and varied little among on-shelf locations but declined rapidly beyond the shelf edge (depth > 300 m; Fig. 3). Due to the uniformity of predicted probabilities on the shelf (Fig. 3A), CPUE and density (CPUE scaled by probability of occurrence) had almost identical patterns, differing only in absolute value (2% lower), and with regards to depth gradient (steeper for density; Fig. 3). An average density of 1.6 tonnes/km^2 (95% CI: 1.2–2.0; Table 4) was predicted across locations where icefish were predicted to occur, with generally higher densities toward shelf edge locations (Fig. 3). Notable high-density areas (density > 10 tonnes/km^2) were predicted on Shag Rocks, and at several locations (northwest, southwest, northeast) on the South Georgia shelf (Fig. 3). Lowest densities were predicted in the southeast sector (0.86 tonnes/km^2; Table 4).

Comparatively, model predictions closely resembled observed CPUE (mean, all-surveys) (Fig. 3). However, high predicted values in the southwest sector were less apparent in observed CPUE, potentially linked to lower coverage in that area (Fig. 3). Uncertainty in predicted density, expressed via coefficient of variation (CV), averaged (median) 0.41, and was highest (> 2) past the 500 m contour due to lower predicted values (Fig. 3). On the shelf (depth < 300 m), uncertainty was highest at locations south of South Georgia, coincident with areas of least coverage (Fig. 3).

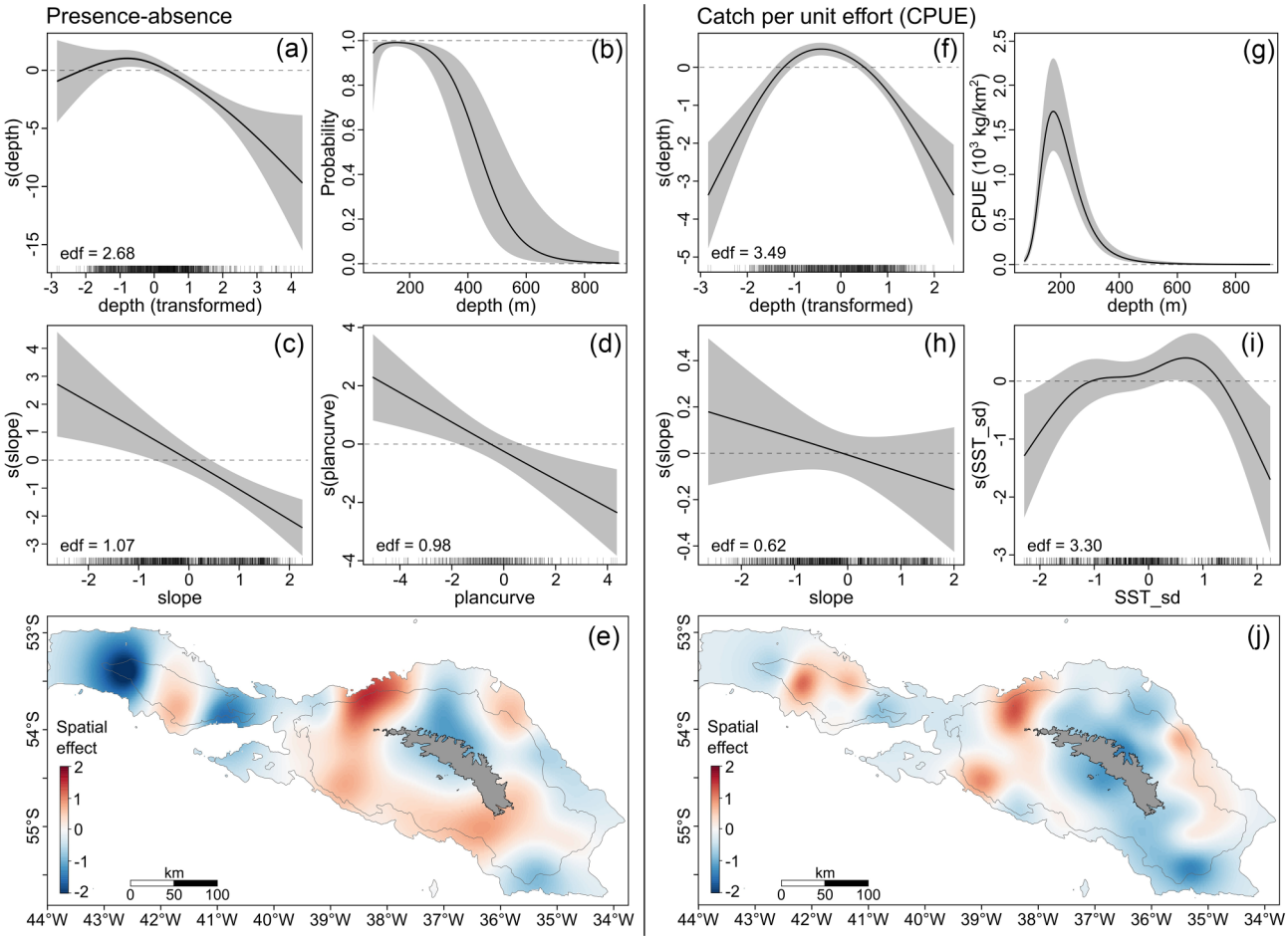

Figure 2. Hurdle model results fitted to mackerel icefish (*Champsocephalus gunnari*) trawl data collected around South Georgia. Presence-absence (**A–E**) and log-transformed catch-per-unit effort (CPUE; **F–J**) model components are shown for the best fitting model. Presence-absence model results show the fitted relationship for depth, shown on the link/transformed scale (**A**) and when back-transformed to natural units (**B**), seabed slope (**C**), seabed planform curvature (**D**) and spatial effects (**E**). CPUE model results are shown for depth on the model (log-CPUE, transformed depth; **F)** and backtransformed (**G**) scales, seabed slope (**H**), variation in sea surface temperature (SST_sd; **I**), and spatial effects (**J**). Fitted smooths indicate the mean fitted function with shading representing ± 1 standard error. Smooths included in the best models for sun angle (CPUE: strong positive linear relationship) and mean seafloor dissolved oxygen concentration (presence-absence: weak positive relationship) are omitted to save space. Contour lines on map panels indicate the 500 and 2000 m isobaths.

Investigation of temporal variation in distribution revealed that high CPUE of icefish on the western side of the South Georgia and Shag Rocks shelves were consistent through time (1987–1997, 2000–2010, 2011–2023; Fig. S10). However, CPUE on the northeast South Georgia shelf were more variable, with lower values from 2000–2010, but otherwise high in the earlier and later periods. Taken together, this suggests that the western South Georgia and Shag Rocks shelves constitutes their core area, and that icefish concentrations on the northeast South Georgia shelf are more ephemeral.

Summing model predictions across areas resulted in a long-term average biomass of 63.4 × 10^3 tonnes (95% CI: 49.3–81.7 × 10^3 tonnes), primarily distributed in western sectors around South Georgia (54% of the total) and on Shag Rocks (15% of the total; Table 4).

Proportion of krill in icefish diets

Models of mean krill proportions in icefish stomach contents indicated high interannual variability with smaller effects attributable to spatial variation and fish size (Table 5). The addition of depth and date relationships resulted in either less parsimonious models (depth; higher AIC) or had no effect (date: Table 5). Interannual variability accounted for the majority of variance explained (R^2 = 34.1 for survey effects alone; Table 5), with lowest krill proportions (< 20%) estimated for 2009 and 2021 (Fig. 4). A non-linear relationship was estimated in relation to fish length, suggesting relative krill consumption increases with fish size up to 33 cm before declining for larger sizes (Fig. S7). However, the magnitude of this effect was relatively small, with the proportion of krill only changing by ± 4%–5% across the sampled size range.

From the model containing no spatial components, icefish diets were estimated to contain an average of 60.1% krill by mass (bootstrapped 95% CI: 57.1–63.5%; Table 5). Incorporating spatial variation resulted in reduced AIC and explained an additional 4% (sector) to 7% (spatial field) of variation (Table 5). Sector spatial models indicated higher krill proportions in the northwest sector (67.2%, 95% CI = 63.3–70.6%) than elsewhere on the South Georgia shelf. However, all sectors on the South Georgia shelf had higher proportions than Shag Rocks (48.6%, 95% CI = 42.5–

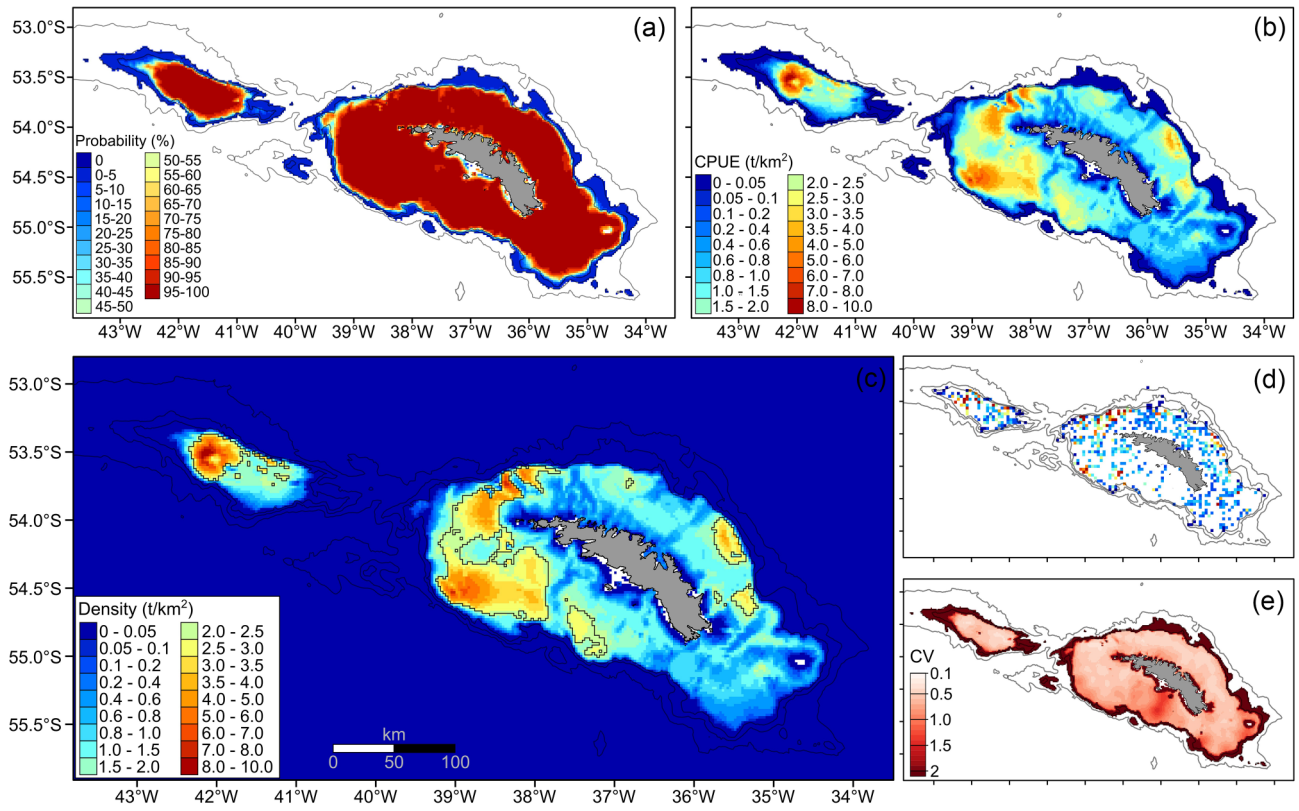

Figure 3. Predicted mackerel icefish (*Champsocephalus gunnari*) distribution around South Georgia. Hurdle model results are shown for predicted catch probability from the best-fitting model for presence absence (**A**) and predicted catch per unit effort (CPUE in kg/km^2) from the best-fitting model for log-transformed CPUE (**B**). Combined hurdle model predictions of mackerel icefish density (kg/km2; **C**) overlaid with polygons (thick black line) to indicate locations constituting 50% of the total biomass. Observed average CPUE, binned to 5 km resolution (**D**) are also provided as a reference. Combined spatial uncertainty is presented as coefficient of variation (CV; **E**) calculated for each grid cell. Model results in (**A**) and (**B**) are truncated at the 1000 m isobath as no observations were collected from greater depths, but densities in (**C**) of 0 were assigned for depths > 1000 m given the mackerel icefish depth range.

54.2; Table 5), where fish, predominantly nototheniids, were more prominent (Fig. 4). The spatial model indicated a south (low) to north (high) gradient in the proportion of krill in icefish diets on the South Georgia shelf, and a southeast (low) to northwest (high) gradient on Shag Rocks (Fig. 4). Model uncertainty was relatively higher on the shelf south of South Georgia (southeast sector: CV = 0.09–0.42, median = 0.17), coincident with lower sample coverage (Fig. 4). Given that stomach contents collected in 2009 and 2021 contained anomalously low proportions of krill, models were re-fitted to data excluding those years. While these models estimated a higher proportion of krill (63.7% compared to 60.1%), spatial patterns were comparable to those found when all years were included (Fig. S8), suggesting that results were minimally influenced by observations from low krill years.

Krill consumption estimates

Combining density estimates and dietary proportions of krill with daily consumption rates (0.5%, 1% and 2% body mass per day) resulted in estimates ranging from 68 × 10^3 (95% CI: 51–88 × 10^3) to 271 × 10^3 (95% CI: 203–352 × 10^3) tonnes of krill consumed by mackerel icefish per year (Table 4).

Relative to the constant diet scenario, including spatial variability in average diet had only a marginal effect on overall consumption, lowering estimates by 2.5% and 5% for sector-based and continuous representations of icefish diets, respectively (Table 4). However, this was largely due to a shift among areas, with consumption estimates dropping by 12%–22% on Shag Rocks when spatial variation was included, and increasing on the South Georgia shelf, particularly in the northwest sector where consumption estimates increased by 10%–11% (Table 4). Based on the spatial diet model, annual consumption estimates per unit area were highest along the shelf edge in the northwest sector due to high density and high proportions of krill in icefish diets, and on the Shag Rocks shelf primarily driven by higher densities, albeit with lower proportional krill consumption (Fig. 5).

Overlap between krill consumption and fishery harvest

Krill fishing from 2004–2023 was concentrated inshore of the 500 m isobath throughout the northwest and northeast sectors around South Georgia, with highest concentrations in the northeast (Fig. 5). The krill fishery footprint (cells contributing 90% of the total catch) overlapped with high relative consumption of krill by mackerel icefish, most notably along the northwest shelf edge where icefish are most abundant and in the northeast sector due to concentrated fishing effort (Fig. 5). Spatial overlap, measured by indices of collocation between icefish consumption and commercial krill catch,

Table 4. Mackerel icefish (Champsocephalus gunnari) estimated biomass and krill consumption on the South Georgia and Shag Rocks shelf.

Measure	Diet scenario	Sector					Total
		Shag Rocks	Northwest	Northeast	Southeast	Southwest	
Area (km^2)[a]		4157	5773	6592	11 560	11 904	**39 986**
Biomass							
Biomass (10^3 t)		9.6 [6.9–13.2]	9.2 [6.9–12.0]	8.7 [6.4–11.3]	9.9 [7.2–13.7]	26.1 [18.7–36.1]	**63.4 [49.3–81.7]**
Mean density (t/km^2)		2.31 [1.66–3.18]	1.59 [1.20–2.08]	1.32 [0.97–1.71]	0.86 [0.62–1.19]	2.19 [1.57–3.03]	**1.58 [1.23–2.04]**
Proportion (by mass) of krill in diet							
Diet: % Krill	Constant						**60.1 [57.1–63.5]**
	Sector	48.6 [42.5–54.2]	67.2 [63.3–70.6]	60.7 [55.1–65.9]	57.0 [49.9–63.6]	60.0 [54.5–65.1]	**58.8 [55.1–62.5]**
	Smooth	50.0 [43.1–56.5]	64.5 [60.0–68.9]	60.0 [53.8–65.7]	52.6 [44.2–62.1]	55.2 [47.3–64.2]	**55.9 [51.2–61.0]**
Krill consumption							
Krill biomass (10^3 t/year)	Constant	20.3 [14.3–27.5]	20.0 [15.0–26.2]	18.5 [14.0–24.2]	22.0 [15.4–29.9]	57.4 [40.4–78.6]	**138.3 [107.9–176.2]**
	Sector	16.4 [11.6–23.1]	22.3 [16.5–29.0]	18.8 [14.1–24.8]	20.8 [15.2–28.3]	57.3 [41.0–78.3]	**135.8 [106.3–172.5]**
	Smooth	18.6 [12.6–26.4]	22.1 [16.3–29.2]	18.5 [13.6–24.5]	20.0 [13.7–28.1]	53.0 [36.3–76.3]	**132.5 [101.4–170.8]**
Spatial overlap (Index of co-location) with commercial krill fishery (2004–2023)							
Spatial overlap (0–1)	Constant	0	0.319 [.271-0.368]	0.380 [.297-0.469]	0.171 [.101-0.258]	0.037 [.019-0.066]	**0.141 [0.104–0.186]**
	Sector	0	0.319 [.271-0.368]	0.380 [.297-0.469]	0.171 [.101-0.258]	0.037 [.019-0.066]	**0.148 [0.108–0.192]**
	Smooth	0	0.322 [.272-0.371]	0.372 [.286-0.464]	0.177 [.098-0.277]	0.035 [.017-0.064]	**0.146 [0.106–0.193]**

[a]: Summed area weighted by predicted probability of occurrence.
Consumption estimates correspond to a daily feeding rate of 1% fish body mass per day. Lower (0.5%) and higher (2%) daily feeding rate scenarios are omitted to save space given they are linearly related (0.5 ×, 2 ×) to those presented for krill consumption. Measures of spatial overlap between icefish krill consumption and the krill fishery are also presented in the form of indices of collocation for each consumption scenario.

Table 5. Statistics for models of proportional krill consumption by mackerel icefish (Champsocephalus gunnari).

Model	df	AIC	R^2
intercept only	7.3	317.7	14.6[a]
survey [12.3]	21.9	154.5	34.1
survey [12.4] + depth [1.5]	23.3	154.7	34.4
survey [12.3] + time [0]	21.9	154.5	34.1
survey [12.4] + fish_length [2.4]	24.4	153.3	34.7
survey [12.4] + sector [3.6]	25.7	120.7	37.7
survey [12.4] + space (NS; 40 km) [16.4]	37.7	102.6	41.2
survey [12.5] + fish_length [2.7] + sector [3.6][b]	28.5	118.7	38.3
survey [12.5] + fish_length [2.7] + depth [1.6] + sector [3.6][b]	29.9	120.0	38.5
survey [12.4] + fish_length [2.3] + space (NS; 40 km) [15.8][c]	39.5	102.0	41.5

[a]: Variance explained by the null model is attributable to that explained by sub-models for 0/1 inflation parameters.
[b]: Smooths for time were added to these models but were effectively removed due to shrinkage, resulting in identical models to those presented.
[c]: Smooths for depth and time were added to this model but were effectively removed due to shrinkage resulting in identical models to those presented.
Results presented relate to alternate structures for the mean parameter (mu) in 0/1 inflated Beta generalized additive models applied to the proportion of Antarctic krill (Euphausia superba) in mackerel icefish stomach contents. Terms trialled were survey random effects (basis = "re"), shrinkage penalized smooths (basis = "ts") for depth, time, and mean fish length, and sector-specific (basis = "re") or gaussian process (basis = "gp") spatial structures. Presented statistics are the model degrees of freedom across mean (mu), variance (sigma), and 0/1 (nu, tau) inflation parameters, Akaike's information criterion (AIC) and the Cox-Snell pseudo R^2 value. For gaussian process models, values are only presented for models with range parameters that resulted in the lowest AIC (range = 40 km; non-stationary). All models had the same structure for variance and 0/1 inflation parameters. Estimated degrees of freedom (EDF) are given in [].

ranged between 0.141 and 0.148, with marginally higher values when accounting for spatial variation in icefish diet (Table 4). To address potential changes in fishing distribution we compared the 2004–2023 map of cumulative krill catch to equivalent maps created by summing krill catch in 5-year blocks. Whilst this revealed a general shift and concentration of fishing effort to the northeast of South Georgia, areas fished in most recent years (2020–2023) were largely coincident with longer-term (2004–2023) patterns (Fig. S11). As such, we believe our results to be broadly representative of current patterns in the distribution of the krill fishery at South Georgia.

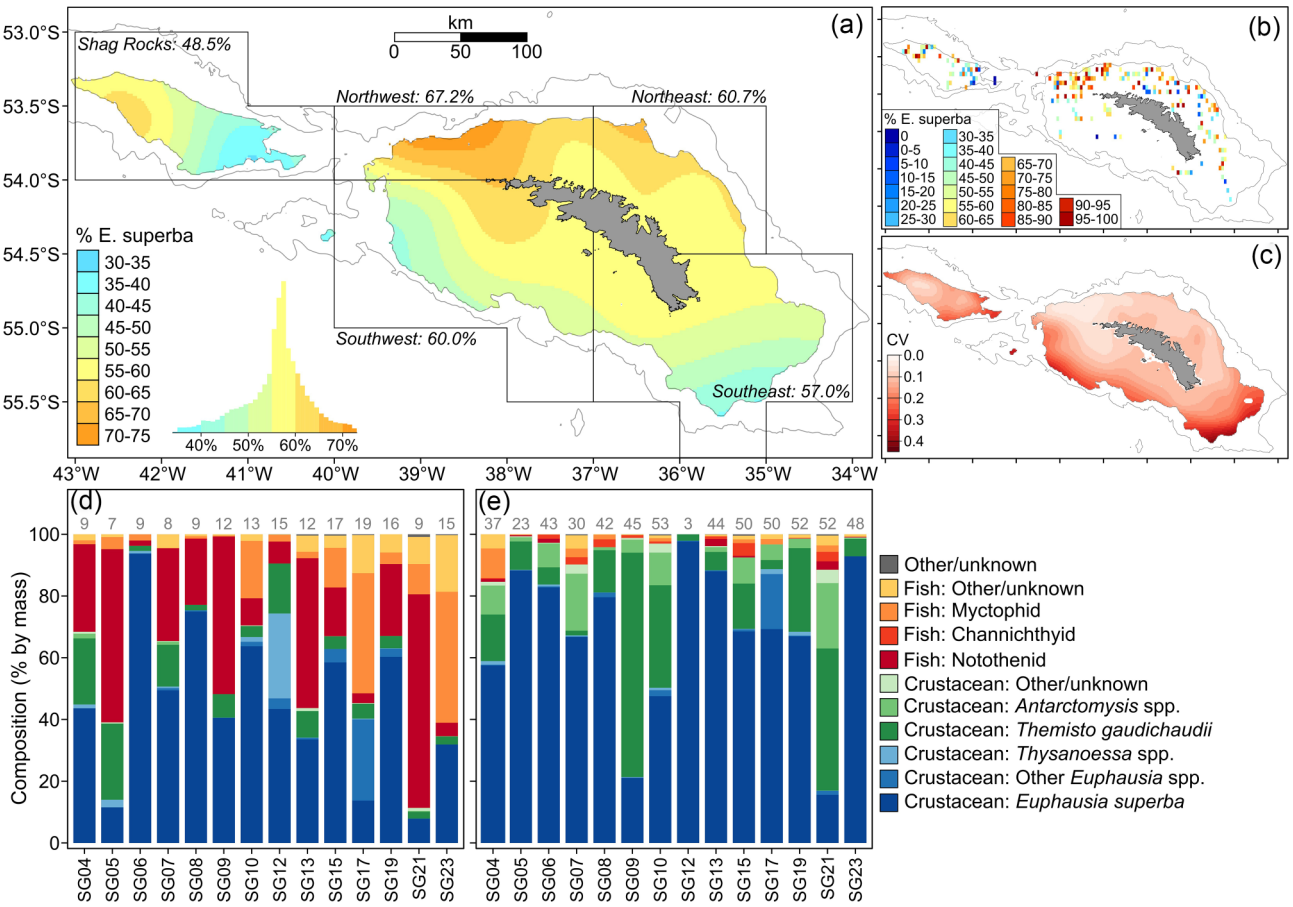

Figure 4. Variation in the proportion of Antarctic krill (*Euphausia superba*) in mackerel icefish (*Champsocephalus gunnari*) diets around South Georgia. Model results from a generalized additive model containing a spatial smooth (**A**) fitted to the proportion of krill in icefish stomach contents. Predictions are constrained to depths less than 500 m given the depth range of trawls with diet samples (0–446 m). Estimated proportions from the sector spatial model are also given for each sector (black polygons in **A**). A representation of the raw data aggregated to a 5 × 5 km grid (**B**) is also given for reference. Uncertainty in spatial smooth model estimates is also presented as the coefficient of variation (CV; **C**) for each grid cell calculated via bootstrap resampling. Temporal variability in gross mackerel icefish diet from 2004–2023 for Shag Rocks (**D**) and South Georgia (**E**). Plotted proportions in (**D**) and (**E**) represent the proportions within each region and year after pooling all fish stomach contents. The number of trawls from which stomach contents were sampled is given by grey text in panels (**D**) and (**E**).

Discussion

Mackerel icefish are the most abundant krill-eating demersal fish on the South Georgia and Shag Rocks shelf and are a priority species when assessing possible ecosystem impacts of krill fishing in this region. Our results are consistent with previous studies (e.g. Everson et al. 1999, Main et al. 2009) that the distribution of mackerel icefish is governed primarily by depth but provides more detailed information on their distribution across the South Georgia shelf. Our diet analyses also indicate spatial variation in relative krill consumption, which may pertain to patterns of krill availability. While our results indicate that overlap between icefish distribution and krill fishing is currently low at South Georgia, our study provides the necessary information to aid future management of the krill fishery to minimize impacts on mackerel icefish.

Mackerel icefish distribution

Excluding depth, habitat covariates explained a relatively small amount of variation in icefish distribution. Among those, seabed slope and planform curvature were both negatively correlated with icefish density. Seabed morphology is frequently associated with demersal fish distributions (Borland et al. 2021), with the negative relationship found for slope demonstrated in other studies on shelf-associated species (Smith and Lindholm 2016, Smoliński and Radtke 2017). The negative relationship found for planform curvature likely indicates higher abundance in canyons on the shelf than would be expected given their absolute depth. Association with marine canyons may be due to prey availability and retention, as Antarctic krill, and euphausiids more broadly, aggregate in marine canyons (Bernard et al. 2017, Santora et al. 2018). Areas of high icefish density were frequently adjacent to canyons that cut into the South Georgia shelf, which may facilitate transport and retention of krill to the shelf-based ecosystem by wind and tidal forcing (Bernard et al. 2017).

Variation in SST was also included in models for CPUE, indicating lower density in locations with low or high SST variability. Whilst temperature may be a limiting factor for icefish physiology, given their northern range limit occurs at Shag Rocks (Morley et al. 2014), we suspect that the fitted relationship is more likely due to location-specific effects, rather than causally related to temperature variation. Extreme high and low values for SST variation that seem to be driving this relationship were highly localized (northwestern edge of the Shag Rocks shelf, and adjacent to the northwest tip of South

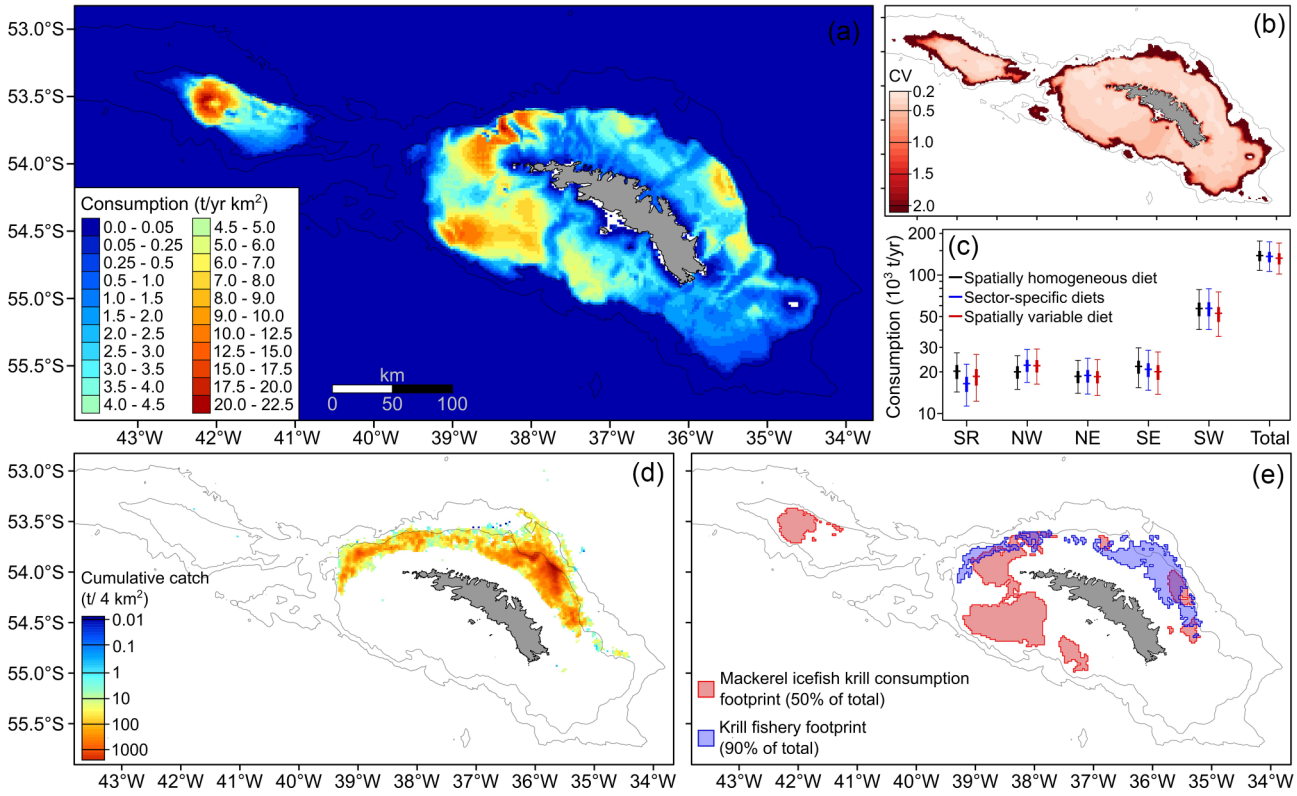

Figure 5. Consumption estimates for mackerel icefish (*Champsocephalus gunnari*) feeding on Antarctic krill (*Euphausia superba*) and overlap with commercial krill fishing operations around South Georgia. The spatial distribution of mean estimated annual krill consumption by mackerel icefish (tonnes/km^2 per year; **A**), and spatial uncertainty (coefficient of variation, CV; **B**), is shown for the combination of the best-fitting hurdle model for density and the continuous spatial model of mackerel icefish diet (% of krill in diet) assuming a feeding rate of 1% body mass per day. Sector and total consumption estimates (**C**) are shown for the three different scenarios of diet variation investigated (constant, sector-specific, and continuous). Plotted values are the mean and 50% (thick line) and 95% (thin line) confidence intervals. The distribution of the krill fishery operating around South Georgia (**D**) is shown as the cumulative catch in tonnes per 2 × 2 km grid cell over the 2004–2023 period. Spatial overlap between mackerel icefish consumption and fisheries extraction of Antarctic krill (**E**) is shown via polygons representing areas that contribute 50% and 90% of the total extraction by icefish and commercial fishing, respectively.

Georgia, respectively; Fig. S12), and constituted only a small proportion of datapoints. As a result, the fitted SST relationship may arise from limited sampling or may be a proxy for other unknown factors that give rise to lower densities at those locations.

The lack of other environmental factors in our models is likely a consequence of the inclusion of a spatial smooth, which was added to better capture icefish distribution, and to account for spatial autocorrelation. However, habitat relationships may be omitted as a result. Excluding spatial effects from model fitting either strengthened the relationships already identified or selected for additional, mostly weak effects (Supplementary materials: Section 9). Therefore, whilst our chosen model doesn't include all environmental relationships, it captures the main factors and performs better at describing patterns in icefish distribution than using habitat covariates alone.

Spatial variability in mackerel icefish diet

High densities of icefish on the northwest South Georgia shelf were coincident with those where krill predominated in icefish diets, suggesting that krill-availability may be a determining factor in structuring icefish distribution. Our models also indicated high icefish abundance in the southwest sector, but this wasn't coincident with higher krill content in icefish diets, but did coincide with higher proportions of *Themisto gaudichaudii*. Apart from Shag Rocks, where fish constitute a larger proportion of icefish diet, *T. gaudichaudii* was the second most important prey source. If *T. gaudichaudii* are consistently available in the southwest, it may explain how relatively high densities of icefish are able to persist there. An alternative interpretation is that krill abundance and/or availability is lower in the southwest, such that *T. gaudichaudii* forms a larger proportion as secondary prey.

Locations of higher krill consumption by icefish coincide with locations frequented by other krill-dependent predators, including Antarctic fur seals (*Arctocephalus gazella*; Staniland et al. 2011), macaroni penguins (*Eudyptes chrysolophus*; Trathan et al. 2006), and gentoo penguins (*Pygoscelis papua*; Ratcliffe et al. 2021) suggesting a preference for areas where prey are consistently available by multiple taxa. Co-occurrence of multiple krill predators likely increases interspecific competition and localized depletion of krill, which may be exacerbated by krill fishing (Bertrand et al. 2012). Furthermore, in years of low krill availability, prey switching by fur seals towards greater consumption of mackerel icefish impact icefish via bottom-up (loss of krill prey) and top-down (increased predation by fur seals) effects (Everson et al. 1999, Hill et al. 2012). Taken together, knowledge of the distribution of the suite of krill predators can inform precautionary management of the fishery to avoid exacerbating the direct

(i.e. prey resource limitation) and indirect (i.e. prey-switching) consequences of natural variation in krill abundance.

Biomass and total krill consumption estimates

Distribution models for mackerel icefish at South Georgia indicated a long-term average biomass of 63 × 10^3 tonnes (henceforth, kt). However, our density estimates are almost certainly an underestimate as they do not account for icefish in the water column (Everson et al. 1996) above the trawl headline height (3-6 m). Furthermore, catchability of mackerel icefish near the seabed (i.e. available to trawl gear) is likely also less than one, introducing further bias that may vary among years according to population size structure (Fraser et al. 2007) given omission of small fish due to mesh size (40 mm). Studies investigating mackerel icefish predator (gentoo penguins and fur seals) diets at South Georgia are suggestive of annual consumption of icefish exceeding 100kt per year (Reid et al. 2005). Additionally, ecosystem models for South Georgia suggest that mackerel icefish biomass up to ten-times higher than bottom-trawl survey estimates is needed to satisfy the requirements of the pelagic food web (Hill et al. 2012).

Our models were suggestive of diel vertical migration according to time of day indicating higher biomass near the seabed towards noon. These results are consistent with icefish tracking diel-vertical migration of krill (Bahlburg et al. 2023). However, the magnitude of this effect (1.5 × difference between dawn and midday) is small relative to the discrepancy between our estimated biomass and that indicated by consumption rates of icefish predators. Taken further, this suggests a potentially large proportion of the population are dispersed throughout the water column at all times of day.

Krill consumption by mackerel icefish using our median estimate of consumption rate (1% body mass per day) was estimated at 133kt per year, with some locations exceeding 20 tonnes per km^2 per year. Given that biomass is potentially ∼2–10 times higher than our estimate, it is likely that mackerel icefish are a major consumer of krill both at local- and regional-scales. Inclusion of spatial variability in diet had little effect on gross consumption estimates but did place greater emphasis on areas that the fishery operates in, notably to the northwest of South Georgia. The northwest shelf is also a major foraging area for other krill consuming taxa, notably fur seals, and gentoo and macaroni penguins (Trathan et al. 2006, Staniland et al. 2011, Ratcliffe et al. 2021). Boyd (2002) estimated that macaroni penguin consume 8 million tonnes (Mt) of krill per year at South Georgia, which when adjusted for current population estimates (∼ 1 million pairs compared to 3 million pairs) suggests consumption of ∼2.7Mt per year. The fur seal population at South Georgia may consume ∼3.8Mt per year (Boyd 2002), based on the 1991 population estimate of 1.55 million animals that is comparable to current estimates following population increases and subsequent declines since 1991 (Forcada et al. 2023). Comparatively, gentoo penguins, numbering ∼100 000 breeding pairs on South Georgia (Herman et al. 2020) are estimated to consume ∼45kt per year (Williams 1991). Average annual consumption of krill by mackerel icefish likely exceeds that of gentoo penguins and may be of the same order of magnitude as that of fur seals and macaroni penguins dependent on the bias in our estimate of icefish biomass. In addition, increased icefish biomass following years of strong recruitment and survival may well increase consumption to well above the long-term average in particular years. Estimates of interannual variability, based on survey random effects from the CPUE model, suggest that icefish densities vary from 0.3 × to 3.4 × the long-term mean (± 2 standard deviations of survey random effects after conversion from log- to natural-scale) among years. However, realized interannual variation in biomass is likely lower, as survey differences incorporate natural variation in biomass in addition to variation in sampling among surveys and may be affected by singular trawls when they encounter large aggregations (i.e. high CPUE in 1990 and 2013 were due to individual trawls capturing 37 tonnes and 24 tonnes of icefish, respectively, each accounting for more than 50% of the survey total). Despite that, short-term variability in demersal fish populations, and consequently krill requirements, ought to be a higher priority for consideration in krill fishery management when compared to other krill consumers, such as fur seals or penguins, whose populations vary less among years.

Our consumption estimates are, however, based on uncertain estimates of daily feeding rates. Whilst feeding rates of up to 2% body mass per day have been recorded for mackerel icefish (Kock et al. 2012), these may be under ideal conditions of abundant prey and zero competition. Daily feeding rates of 1% body mass per day when annualized (i.e. Q/B = 3.65) exceeds those used in ecosystem models for mackerel icefish at South Georgia (Q/B = 1.9; Hill et al. 2012) and for demersal fish in the Ross Sea (Q/B = 1.89; Pinkerton et al. 2010) and the Western Antarctic Peninsula (Q/B = 2; Ballerini et al. 2014). They also exceed those estimated for gadiform fish in northern hemisphere high-latitude ecosystems (Q/B = 2–2.713; Whitehouse et al. 2014, Bentley et al. 2017). Taken together, this suggests that estimates corresponding to 0.5% body mass per day are more likely. Therefore, we suggest that krill consumption of 62kt per year represents an absolute minimum, but that realized consumption is potentially an order of magnitude higher given biased estimates of biomass.

Given uncertainties in biomass and feeding rate, we advise that our estimates of krill consumption are only applied alongside some appreciation of the potential magnitude of those biases. Addressing our major concern, that icefish biomass is underestimated by demersal trawl sampling, will require approaches such as concurrent acoustic sampling (Godø and Wespestad 1993, McQuinn et al. 2005, Kotwicki et al. 2018) to identify the vertical distribution of icefish in the water column, as well as studies investigating net avoidance behaviour (Doray et al. 2010). Acoustic sampling may also help to identify patches of high icefish density (i.e. Everson et al. 1996) that could be used in sampling design to obtain more accurate and precise estimates of biomass (McQuinn et al. 2005); however, this would also require studies to further refine the acoustic characteristics of icefish to distinguish them from krill and other semi-pelagic species (Fallon et al. 2016). Refining feeding rate estimates, by collecting additional data from South Georgia across different seasons, or via alternate approaches such as those based on metabolic rates (Johnston and Battram 1993), would help to ascertain whether feeding rates vary seasonally, or in accordance with prey availability or composition (Pedersen 2000). We also implicitly assume that icefish distributions are similar year-round, as we have insufficient data outside of the summer survey period (December-February). Additional trawl surveys at other times of year may enable the development of seasonal distribution models, as well as to identify seasonal variation in diet if concurrent stomach

content sampling were to be performed. However, in the near-term, these data are unlikely to become available within the timeframe needed to inform krill fishery management. As an interim measure, we would propose that krill consumption by mackerel icefish be included in the krill fishery management evaluation via multiple scenarios, such as by scaling predicted distributions in accordance with ecosystem model (i.e. Hill et al. 2012) or predator diet (Reid et al. 2005) estimates of total biomass and evaluating the impact on spatial management outcomes. This type of sensitivity analysis, if also applied across other krill-dependent species considered in the krill fishery management approach (Warwick-Evans et al. 2022a, b), would help to ensure that decisions are made given the data currently available, while acknowledging key sources of uncertainty.

Overlap with the krill fishery

Given that the krill fishery operates exclusively during winter around South Georgia (Trathan et al. 2021), penguins and fur seals that are highly mobile may be more able to adapt to localized depletions of krill, than less mobile demersal fish. Our assessment of relative overlap between the fishery and icefish consumption indicated relatively low overlap due to high icefish abundance in areas where fishing does not currently occur (south of South Georgia) or is prohibited (within 22 km of Shag Rocks), and the relative concentration of fishing effort. Despite current low overlap, our results provide the foundation for including demersal fish in the future development of krill fishery management at South Georgia. Furthermore, our study illustrates the data and methods required to evaluate overlap between demersal fish and the krill fishery, which could be applied elsewhere, such as at the Western Antarctic Peninsula and South Orkney Islands where the krill fishery is more active (Trathan et al. 2021).

Conclusion

Our study represents one of the few to examine the fine-scale distribution of a demersal fish species in the Southern Ocean. Furthermore, our exploration of spatial variability in diet represents an important consideration for icefish ecology and the potential availability of krill to predators on the South Georgia shelf. Whilst our study demonstrates that spatial overlap between icefish and krill fishing is currently low at South Georgia, present management of the krill fishery allows for significant spatial and seasonal concentration of krill catch, raising the risk to krill-dependent predators at targeted locations. Re-establishment of spatial management, incorporating spatial information on krill consumption by both resident (demersal fish, gentoo penguins, fur seals) and seasonally abundant (macaroni penguins, cetaceans) taxa, is therefore critical to minimize the potential for adverse impacts to krill-dependent predator populations.

Acknowledgements

The authors thank the crews, vessel owners, scientists and observers involved in collecting groundfish data and the krill fishing industry and CCAMLR secretariat for provision of catch information.

Author contributions

Timothy Jones (Conceptualization [equal], Data curation [equal], Formal Analysis [lead], Investigation [lead], Methodology [lead], Software [lead], Visualization [lead], Writing—original draft [lead], Writing—review & editing [lead]), Victoria Warwick-Evans (Conceptualization [equal], Funding acquisition [equal], Investigation [supporting], Project administration [lead], Writing—original draft [supporting], Writing—review & editing [supporting]), Simeon Hill (Conceptualization [equal], Investigation [supporting], Writing—original draft [supporting], Writing—review & editing [supporting]), Martin Collins (Conceptualization [equal], Data curation [lead], Investigation [supporting], Writing—original draft [supporting], Writing—review & editing [supporting]).

Supplementary data

Supplementary data is available at *ICES Journal of Marine Science* is available at *ICES Journal of Marine Science* online.

Conflict of interest: The authors declare no conflict of interest.

Funding

M.A.C., S.L.H., and V.W.E. were supported by the NERC-funded CONSEC program at the British Antarctic Survey (BAS) as part of the Polar Science for a Sustainable Planet science strategy. T.J. was supported by the UK Government's Blue Belt Program. Groundfish surveys used in this study were funded by the Government of South Georgia and the South Sandwich Islands (GSGSSI) and the King Edward Point Science Programme was jointly funded by the UK FCDO and GSGSSI.

Data availability statement

The data underlying this article are available on Zenodo at https://doi.org/10.5281/zenodo.15125451 and are publicly available.

References

Bahlburg D, Hüppe L, Böhrer T *et al.* Plasticity and seasonality of the vertical migration behaviour of Antarctic krill using acoustic data from fishing vessels. *R Soc Open Sci* 2023;**10**:p.230520. https://doi.org/10.1098/rsos.230520

Ballerini T, Hofmann EE, Ainley DG *et al.* Productivity and linkages of the food web of the southern region of the western Antarctic Peninsula continental shelf. *Prog Oceanogr* 2014;**122**:10–29. https://doi.org/10.1016/j.pocean.2013.11.007

Bentley JW, Serpetti N, Heymans JJ. Investigating the potential impacts of ocean warming on the Norwegian and Barents Seas ecosystem using a time-dynamic food-web model. *Ecol Modell*, 2017;**360**:94–107. https://doi.org/10.1016/j.ecolmodel.2017.07.002

Berger AM, Deroba JJ, Bosley KM *et al.* Incoherent dimensionality in fisheries management: consequences of misaligned stock assessment and population boundaries. *ICES J Mar Sci* 2021;**78**:155–71. https://doi.org/10.1093/icesjms/fsaa203

Bernard KS, Cimino M, Fraser W *et al.* Factors that affect the nearshore aggregations of Antarctic krill in a biological hotspot. *Deep Sea Res Part I* 2017;**126**:139–47. https://doi.org/10.1016/j.dsr.2017.05.008

Bertrand S, Joo R, ArbuluSmet C *et al.* Local depletion by a fishery can affect seabird foraging. *J Appl Ecol* 2012;**49**:1168–77. https://doi.org/10.1111/j.1365-2664.2012.02190.x

Borland HP, Gilby BL, Henderson CJ *et al.* The influence of seafloor terrain on fish and fisheries: a global synthesis. *Fish and Fisheries* 2021;**22**:707–34. https://doi.org/10.1111/faf.12546

Boyd IL. Estimating food consumption of marine predators: antarctic fur seals and macaroni penguins. *J Appl Ecol*, 2002;**39**:103–19. https://doi.org/10.1046/j.1365-2664.2002.00697.x

Canseco JA, Alegría N, Niklitschek EJ. Consumption of Antarctic krill *Euphausia superba* by mackerel icefish, *Champsocephalus gunnari* off the South Orkney Islands: filling an information gap in the current ecosystem-based management approach. *Polar Biology*, 2024;**47**:989–1000. https://doi.org/10.1007/s00300-024-03270-9

Carroll G, Holsman KK, Brodie S *et al.* A review of methods for quantifying spatial predator–prey overlap. *Global Ecol Biogeogr* 2019;**28**:1561–77. https://doi.org/10.1111/geb.12984

CCAMLR. *Scientific committee for the conservation of Antarctic marine living resources, in Report of the thirty-eighth meeting of the scientific committee*. (Hobart, Australia: CCAMLR), 2019

Constable AJ, Kawaguchi S, Sumner M *et al.* A dynamic framework for assessing and managing risks to ecosystems from fisheries: demonstration for conserving the krill-based food web in Antarctica. *Frontiers in Ecology and Evolution* 2023;**11**:p.1043800. https://doi.org/10.3389/fevo.2023.1043800

Doray M, Mahevas S, Trenkel VM. Estimating gear efficiency in a combined acoustic and trawl survey, with reference to the spatial distribution of demersal fish. *ICES J Mar Sci*, 2010;**67**:668–76. https://doi.org/10.1093/icesjms/fsp277

Dormann CF, Elith J, Bacher S *et al.* Collinearity: a review of methods to deal with it and a simulation study evaluating their performance. *Ecography* 2013;**36**:27–46. https://doi.org/10.1111/j.1600-0587.2012.07348.x

Evans JS, Murphy MA. spatialEco. R package version 2.0-2, 2023https://github.com/jeffreyevans/spatialEco (24 June 2024, date last accessed).

Everson I, Bravington M, Goss C. A combined acoustic and trawl survey for efficiently estimating fish abundance. *Fish Res*, 1996;**26**:75–91. https://doi.org/10.1016/0165-7836(95)00404-1

Everson I, Parkes G, Kock KH *et al.* Variation in standing stock of the mackerel icefish *Champsocephalus gunnari* at South Georgia. *J Appl Ecol* 1999;**36**:591–603. https://doi.org/10.1046/j.1365-2664.1999.00425.x

Falco FL, Preiss-Bloom S, Dayan T. Recent evidence of scale matches and mismatches between ecological systems and management actions. *Current Landscape Ecology Reports*, 2022;**7**:104–15. https://doi.org/10.1007/s40823-022-00076-5

Fallon NG, Fielding S, Fernandes PG. Classification of Southern Ocean krill and icefish echoes using random forests. *ICES J Mar Sci*, 2016;**73**:1998–2008. https://doi.org/10.1093/icesjms/fsw057

Fielding S, Watkins JL, Trathan PN *et al.* Interannual variability in Antarctic krill (*Euphausia superba*) density at South Georgia, Southern Ocean: 1997–2013. *ICES J Mar Sci* 2014;**71**:2578–88. https://doi.org/10.1093/icesjms/fsu104

Forcada J, Hoffman JI, Gimenez O *et al.* Ninety years of change, from commercial extinction to recovery, range expansion and decline for Antarctic fur seals at South Georgia. *Global Change Biol* 2023;**29**:6867–87. https://doi.org/10.1111/gcb.16947

Fraser HM, Greenstreet SP, Piet GJ. Taking account of catchability in groundfish survey trawls: implications for estimating demersal fish biomass. *ICES J Mar Sci*, 2007;**64**:1800–19. https://doi.org/10.1093/icesjms/fsm145

Godø OR, Wespestad VG. Monitoring changes in abundance of gadoids with varying availability to trawl and acoustic surveys. *ICES J Mar Sci*, 1993;**50**:39–51.

Griffiths SP, Olson RJ, Watters GM. Complex wasp-waist regulation of pelagic ecosystems in the Pacific Ocean. *Reviews in Fish Biology and Fisheries*, 2013;**23**:459–75. https://doi.org/10.1007/s11160-012-9301-7

Heagerty PJ, Zheng Y. Survival model predictive accuracy and ROC curves. *Biometrics*, 2005;**61**:92–105. https://doi.org/10.1111/j.0006-341X.2005.030814.x

Herman R, Borowicz A, Lynch M *et al.* Update on the global abundance and distribution of breeding Gentoo Penguins (*Pygoscelis papua*). *Polar Biology* 2020;**43**:1947–56. https://doi.org/10.1007/s00300-020-02759-3

Hijmans RJ. raster: Geographic data analysis and modeling. R package version 3.6-32, 2025. https://rspatial.org/raster. (07 May 2025, date last accessed).

Hill SL, Hinke J, Bertrand S *et al.* Reference points for predators will progress ecosystem-based management of fisheries. *Fish and Fisheries* 2020;**21**:368–78. https://doi.org/10.1111/faf.12434

Hill SL, Keeble K, Atkinson A *et al.* A foodweb model to explore uncertainties in the South Georgia shelf pelagic ecosystem. *Deep Sea Res Part II* 2012;**59-60**:237–52. https://doi.org/10.1016/j.dsr2.2011.09.001

Hill SL, Reid K, Thorpe SE *et al.* A compilation of parameters for ecosystem dynamics models of the Scotia Sea-Antarctic Peninsula region. *CCAMLR Science* 2007;**14**:1–25.

Johnston IA, Battram J. Feeding energetics and metabolism in demersal fish species from Antarctic, temperate and tropical environments. *Mar Biol*, 1993;**115**:7–14. https://doi.org/10.1007/BF00349380

Kammann EE, Wand MP. Geoadditive models. *Journal of the Royal Statistical Society Series C: Applied Statistics*, 2003;**52**:1–18. https://doi.org/10.1111/1467-9876.00385

Kock KH. Antarctic icefishes (Channichthyidae): a unique family of fishes. *Polar Biology*, 2005;**28**:862–95. https://doi.org/10.1007/s00300-005-0019-z

Kock KH, Barrera-Oro E, Belchier M *et al.* The role of fish as predators of krill (*Euphausia superba*) and other pelagic resources in the Southern Ocean. *CCAMLR Science* 2012;**19**:115–69.

Kock KH, Everson I. Biology and ecology of mackerel icefish, *Champsocephalus gunnari*: an Antarctic fish lacking hemoglobin. *Comp Biochem Physiol A Physiol*, 1997;**118**:1067–77. https://doi.org/10.1016/S0300-9629(97)86795-3

Kotwicki S, Ressler PH, Ianelli JN *et al.* Combining data from bottom-trawl and acoustic-trawl surveys to estimate an index of abundance for semipelagic species. *Can J Fish AquatSci* 2018;**75**:60–71. https://doi.org/10.1139/cjfas-2016-0362

Main CE, Collins MA, Mitchell R *et al.* Identifying patterns in the diet of mackerel icefish (*Champsocephalus gunnari*) at South Georgia using bootstrapped confidence intervals of a dietary index. *Polar Biology* 2009;**32**:569–81. https://doi.org/10.1007/s00300-008-0552-7

Marra G, Wood SN. Practical variable selection for generalized additive models. *Comput Stat Data Anal*, 2011;**55**:2372–87. https://doi.org/10.1016/j.csda.2011.02.004

McQuinn IH, Simard Y, Stroud TWF *et al.*. An adaptive, integrated "acoustic trawl" survey design for Atlantic cod (*Gadus morhua*) with estimation of the acoustic and trawl dead zones. *ICES J Mar Sci* 2005;**62**:93–106. https://doi.org/10.1016/j.icesjms.2004.06.023

Morley SA, Belchier M, Sands C *et al.* Geographic isolation and physiological mechanisms underpinning species distributions at the range limit hotspot of South Georgia. *Reviews in fish biology and fisheries* 2014;**24**:485–92. https://doi.org/10.1007/s11160-013-9308-8

Murphy EJ, Watkins JL, Meredith MP *et al.* Southern Antarctic Circumpolar Current Front to the northeast of South Georgia: horizontal advection of krill and its role in the ecosystem. *J Geophys Res: Oceans* 2004;**109**:C01029. https://doi.org/10.1029/2002JC001522

Murphy EJ, Watkins JL, Trathan PN *et al.* Spatial and temporal operation of the Scotia Sea ecosystem: a review of large-scale links in a krill centred food web. *Philosophical Transactions of the Royal Society B: Biological Sciences* 2007;**362**:113–48. https://doi.org/10.1098/rstb.2006.1957

Naylor RL, Kishore A, Sumaila UR *et al.* Blue food demand across geographic and temporal scales. *Nat Commun* 2021;**12**:5413. https://doi.org/10.1038/s41467-021-25516-4

Nicol S, Foster J. The fishery for Antarctic krill: its current status and management regime. *Biology and ecology of Antarctic krill* 2016:387–421.

NOAA National Centers for Environmental Information. *ETOPO 2022 15 Arc-Second Global Relief Model*. NOAA National Cen-

ters for Environmental Information, 2022https://doi.org/10.25921/fd45-gt74. (3 March 2024, date last accessed).
Pauly D, Watson R, Alder J. Global trends in world fisheries: impacts on marine ecosystems and food security. *Philosophical Transactions of the Royal Society B: Biological Sciences*, 2005;**360**:5–12. https://doi.org/10.1098/rstb.2004.1574
Pedersen J. Food consumption and daily feeding periodicity: comparison between pelagic and demersal whiting in the North Sea. *J Fish Biol*, 2000;**57**:402–16. https://doi.org/10.1111/j.1095-8649.2000.tb02180.x
Petza D, Katsanevakis S. Science-informed recommendations to enhance the effectiveness of area-based fisheries management for fisheries sustainability and marine conservation: a global mini-review. *Fish Res*, 2024;**272**:p.106947. https://doi.org/10.1016/j.fishres.2024.106947
Pinkerton MH, Bradford-Grieve JM, Hanchet SM. A balanced model of the food web of the Ross Sea, Antarctica. *CCAMLR Science*, 2010;**17**:1–31.
R Core Team. *R: A Language and Environment for Statistical Computing*. R Foundation for Statistical Computing, Vienna, Austria, 2024https://www.R-project.org/. (14 February 2024, date last accessed).
Ratcliffe N, Deagle B, Love K *et al.* Changes in prey fields increase the potential for spatial overlap between gentoo penguins and a krill fishery within a marine protected area. *Diversity and Distributions* 2021;**27**:552–63. https://doi.org/10.1111/ddi.13216
Reid K, Hill SL, Diniz TC *et al.* Mackerel icefish *Champsocephalus gunnari* in the diet of upper trophic level predators at South Georgia: implications for fisheries management. *Marine Ecology Progress Series* 2005;**305**:153–61. https://doi.org/10.3354/meps305153
Reid K, Watkins JL, Murphy EJ *et al.* Krill population dynamics at South Georgia: implications for ecosystem-based fisheries management. *Marine Ecology Progress Series* 2010;**399**:243–52. https://doi.org/10.3354/meps08356
Rigby RA, Stasinopoulos DM. Generalized additive models for location, scale and shape. *Journal of the Royal Statistical Society Series C: Applied Statistics*, 2005;**54**:507–54. https://doi.org/10.1111/j.1467-9876.2005.00510.x
Santora JA, Schroeder ID, Field JC *et al.* Spatio-temporal dynamics of ocean conditions and forage taxa reveal regional structuring of seabird–prey relationships. *Ecol Appl* 2014;**24**:1730–47. https://doi.org/10.1890/13-1605.1
Santora JA, Zeno R, Dorman JG *et al.* Submarine canyons represent an essential habitat network for krill hotspots in a Large Marine Ecosystem. *Sci Rep* 2018;**8**:p.7579. https://doi.org/10.1038/s41598-018-25742-9
Smith JG, Lindholm J. Vertical stratification in the distribution of demersal fishes along the walls of the La Jolla and Scripps submarine canyons, California, USA. *Cont Shelf Res*, 2016;**125**:61–70. https://doi.org/10.1016/j.csr.2016.07.001
Smoliński S, Radtke K. Spatial prediction of demersal fish diversity in the Baltic Sea: comparison of machine learning and regression-based techniques. *ICES J Mar Sci*, 2017;**74**:102–11.
Staniland IJ, Morton A, Robinson SL *et al.* Foraging behaviour in two Antarctic fur seal colonies with differing population recoveries. *Marine Ecology Progress Series* 2011;**434**:183–96. https://doi.org/10.3354/meps09201
Trathan P, Friedlaender A, Johnson C *et al.* The fishery for Antarctic krill–Conflicts between industrial production, protection of biodiversity, and legal governance. *Mar Policy* 2025;**180**:p.106787. https://doi.org/10.1016/j.marpol.2025.106787
Trathan PN, Fielding S, Hollyman PR *et al.* Enhancing the ecosystem approach for the fishery for Antarctic krill within the complex, variable, and changing ecosystem at South Georgia. *ICES J Mar Sci* 2021;**78**:2065–81. https://doi.org/10.1093/icesjms/fsab092
Trathan PN, Green C, Tanton J *et al.* Foraging dynamics of macaroni penguins *Eudyptes chrysolophus* at South Georgia during brood-guard. *Marine Ecology Progress Series* 2006;**323**:239–51. https://doi.org/10.3354/meps323239
Warwick-Evans V, Constable A, Dalla Rosa L *et al.* Using a risk assessment framework to spatially and temporally spread the fishery catch limit for Antarctic krill in the west Antarctic Peninsula: a template for krill fisheries elsewhere. *Frontiers in Marine Science* 2022a;**9**:p.1015851. https://doi.org/10.3389/fmars.2022.1015851
Warwick-Evans V, Kelly N, Dalla Rosa L *et al.*. Using seabird and whale distribution models to estimate spatial consumption of krill to inform fishery management. *Ecosphere* 2022;**13**, p.e4083. https://doi.org/10.1002/ecs2.4083
Warwick-Evans V, Ratcliffe N, Lowther AD *et al.* Using habitat models for chinstrap penguins *Pygoscelis antarctica* to advise krill fisheries management during the penguin breeding season. *Diversity and Distributions* 2018;**24**:1756–71. https://doi.org/10.1111/ddi.12817
Watters GM, Hinke JT. Conservation in the Scotia Sea in light of expiring regulations and disrupted negotiations. *Conserv Biol*, 2022;**36**:e13925. https://doi.org/10.1111/cobi.13925
Watters GM, Hinke JT, Reiss CS. Long-term observations from Antarctica demonstrate that mismatched scales of fisheries management and predator-prey interaction lead to erroneous conclusions about precaution. *Sci Rep*, 2020;**10**:p.2314. https://doi.org/10.1038/s41598-020-59223-9
Wells BK, Santora JA, Bizzarro JJ *et al.* Trophoscapes of predatory fish reveal biogeographic structuring of spatial dietary overlap and inform fisheries bycatch patterns. *Marine Ecology Progress Series* 2024;**741**:47–70. https://doi.org/10.3354/meps14319
Whitehouse GA, Aydin K, Essington TE *et al.* A trophic mass balance model of the eastern Chukchi Sea with comparisons to other high-latitude systems. *Polar Biology* 2014;**37**:911–39. https://doi.org/10.1007/s00300-014-1490-1
Williams TD. Foraging ecology and diet of gentoo penguins *Pygoscelis papua* at South Georgia during winter and an assessment of their winter prey consumption. *Ibis*, 1991;**133**:3–13. https://doi.org/10.1111/j.1474-919X.1991.tb04803.x
Wood SN. Fast stable direct fitting and smoothness selection for generalized additive models. *Journal of the Royal Statistical Society Series B: Statistical Methodology*, 2008;**70**:495–518. https://doi.org/10.1111/j.1467-9868.2007.00646.x
Wood SN. Fast stable restricted maximum likelihood and marginal likelihood estimation of semiparametric generalized linear models. *Journal of the Royal Statistical Society Series B: Statistical Methodology*, 2011;**73**:3–36https://doi.org/10.1111/j.1467-9868.2010.00749.x

Handling editor: Olav Rune Godø